

AN EXPONENTIAL WAVE INTEGRATOR PSEUDOSPECTRAL METHOD FOR THE SYMMETRIC REGULARIZED-LONG-WAVE EQUATION*

Xiaofei Zhao

IRMAR, Université de Rennes 1, Rennes, 35042, France

Email: zhxfnus@gmail.com

Abstract

An efficient and accurate exponential wave integrator Fourier pseudospectral (EWI-FP) method is proposed and analyzed for solving the symmetric regularized-long-wave (SRLW) equation, which is used for modeling the weakly nonlinear ion acoustic and space-charge waves. The numerical method here is based on a Gautschi-type exponential wave integrator for temporal approximation and the Fourier pseudospectral method for spatial discretization. The scheme is fully explicit and efficient due to the fast Fourier transform. Numerical analysis of the proposed EWI-FP method is carried out and rigorous error estimates are established without CFL-type condition by means of the mathematical induction. The error bound shows that EWI-FP has second order accuracy in time and spectral accuracy in space. Numerical results are reported to confirm the theoretical studies and indicate that the error bound here is optimal.

Mathematics subject classification: 65M12, 65M15, 65M70.

Key words: Symmetric regularized-long-wave equation, Exponential wave integrator, Pseudospectral method, Error estimate, Explicit scheme, Large step size.

1. Introduction

The symmetric regularized long wave (SRLW) equation reads,

$$u_t + \rho_x - u_{xxt} + \frac{1}{2}(u^2)_x = 0, \quad (1.1a)$$

$$\rho_t + u_x = 0, \quad x \in \mathbb{R}, \quad t > 0, \quad (1.1b)$$

$$u(x, 0) = u_0(x), \quad \rho(x, 0) = \rho_0(x), \quad x \in \mathbb{R}, \quad (1.1c)$$

where $u(x, t)$, $\rho(x, t)$ are two real-valued functions, and u_0 , ρ_0 are the given initial data. The equation is widely used for modeling the weakly nonlinear ion acoustic and space-charge waves [14, 23, 25, 26], and was first derived by C. E. Seyler and D. L. Fenstermacher in 1984 in [26] when they were working on a weakly nonlinear analysis of the cold-electron plasma equations appropriate for a strongly magnetized nonrelativistic electron beam such that the fluid motion is constrained to one direction. By eliminating ρ from (1.1), the SRLW equation has an equivalent single equation form as

$$u_{tt} - u_{xx} - u_{xxt} + \frac{1}{2}(u^2)_{xt} = 0, \quad x \in \mathbb{R}, \quad t > 0,$$

* Received November 11, 2013 / Revised version received June 15, 2015 / Accepted October 8, 2015 / Published online January 18, 2016 /

which clearly shows that the SRLW equation is a wave type equation and due to this form, (1.1) is usually referred in the literatures as an equation rather than a system. The SRLW equation is symmetric in spatial and temporal derivatives, and is formally very similar to the regularized long wave equation that describes shallow water waves and plasma drift waves [3,4]. In some special physics situations, a dissipative version of SRLW is also proposed and studied in literature such as [28] and the references therein based on the SRLW equation (1.1).

Theoretically, the SRLW equation has gained many attentions. The local and global well-posedness of the SRLW has been studied by B. Guo in [19] and L. Chen in [13], and has been well-established by C. B. Brango in 2012 in [11]. The theoretical results therein indicate that the solutions of the SRLW equation decay very fast to zero at the far field, i.e.

$$\lim_{x \rightarrow \infty} u(x, t) = \lim_{x \rightarrow \infty} \rho(x, t) = 0,$$

at a fixed $t > 0$. The SRLW equation (1.1) has various conservation laws [13,26], such as the *energy*

$$E(u, \rho) := \int_{-\infty}^{\infty} (u^2(x, t) + u_x^2(x, t) + \rho^2(x, t)) dx \equiv E(u_0, \rho_0), \quad (1.2)$$

and the two time *invariants*

$$I(u) = \int_{-\infty}^{\infty} u(x, t) dx \equiv I(u_0), \quad I(\rho) = \int_{-\infty}^{\infty} \rho(x, t) dx \equiv I(\rho_0). \quad (1.3)$$

The energy (1.2) indicates that the two components u and ρ in the SRLW equation stay in different energy spaces. The SRLW equation (1.1) has also been remarkably pointed out to admit the solitary wave solutions (or solitons) [13,26] as

$$u_S(x, t; v, x_0) = \frac{3(v^2 - 1)}{v} \operatorname{sech}^2 \left(\sqrt{\frac{v^2 - 1}{4v^2}} (x - vt + x_0) \right), \quad (1.4a)$$

$$\rho_S(x, t; v, x_0) = \frac{3(v^2 - 1)}{v^2} \operatorname{sech}^2 \left(\sqrt{\frac{v^2 - 1}{4v^2}} (x - vt + x_0) \right), \quad x \in \mathbb{R}, \quad t \geq 0, \quad (1.4b)$$

where $|v| > 1$ is the velocity of the solitons and $x_0 \in \mathbb{R}$ is a shift in space. The importance of solitons in both theoretical studies of nonlinear wave equations and applications in many physical areas is already well demonstrated in [1,2,15]. L. Chen established the stability theory of these solitary waves (1.4) for SRLW equation in [13]. Integrability of the SRLW equation has been investigated in [26], where SRLW equation has been proved to be a nonintegrable system. Since the nonintegrable systems do not have the inverse scattering theory which is known as the superposition for nonlinear equations [29], so the interactions of the solitary waves are inelastic [12] and the dynamics of the SRLW equation are rather complicated analytical issues. Thus numerical methods and simulations are very much needed for the studies of the SRLW system.

For the numerical aspects, many finite difference (FD) time domain methods have been proposed and analyzed in literature. T. Wang etc. considered some conservative FD schemes that conserve the energy and the invariants in a discrete level in [31,32]. However, these conservative schemes are fully implicit and at each step a full nonlinear problem has to be solved very accurately which is quite time-consuming. To improve the efficiency, some semi-implicit FD methods are also proposed in [31] that make the scheme at each time level a linear tri-diagonal

system to solve. Besides the FD methods, high accuracy methods for spatial discretization have also been considered in the literatures. For instance, [19, 35] apply some spectral methods in spatial discretization but with only first order Euler FD method in temporal discretization. In all, the existing numerical methods either call for some time-consuming nonlinear/linear solvers, or have low accuracy order in space or time approximation. Recently, the exponential wave integrators which have been well-developed originally for oscillatory ODEs from molecular dynamics and are known to have many superior properties than the FD integrators as illustrated in [10, 20–22], coupled with trigonometric spectral methods [27] have become very popular for solving dispersive type and wave type partial differential equations such as the nonlinear Schrödinger equations and the nonlinear Klein-Gordon equation. These methods are known for offering high spatial accuracy, efficient explicit schemes without any CFL-type constraints [17, 18, 34] and high resolution capacity in some limit physical regimes [7, 8]. The error estimates of these methods are usually done by energy method which is standard. However to rigorously establish the optimal error bound without a CFL-type condition, is not a mathematically easy task especially for coupled system [9, 18]. Correct energy spaces need to be used for different components in the equations.

This work is devoted to design an exponential wave integrator Fourier pseudospectral (EWI-FP) method which possesses all the good properties as mentioned above for solving the SRLW equation (1.1). We shall firstly adopt the Fourier spectral method for the spatial discretization and then apply a Gautschi-type [20] EWI that has been considered in [7, 10] to integrate the SRLW equation in the Fourier frequency space. The scheme is fully explicit, easy to implement and efficient due to fast discrete Fourier transform. Rigorously finite time error estimates of the proposed EWI-FP method in the energy space are established, where the results show that the EWI-FP method has second order accuracy in time, spectral accuracy in space if the solution is smooth and no CFL-type conditions for the convergence. Thus, the EWI-FP method can take large time steps and mesh sizes in practical computations. Numerical experiments are carried out for confirm the theoretical results.

The rest of the paper is organised as follows. In Section 2, we propose the exponential integrator pseudospectral method. In Section 3, we establish the main error estimate results. Numerical results are reported in Section 4 to confirm the theoretical studies. Some concluding remarks are given in Section 5. Throughout this paper, we adopt the notation $A \lesssim B$ to represent that there exists a generic constant $C > 0$, which is independent of the time step τ (or n) and mesh size h , such that $|A| \leq CB$.

2. Numerical Method

Due to the fast decay of the solutions of SRLW at the far field, for numerical aspects, we truncate the whole space problem onto a finite interval $\Omega = (a, b)$ with periodic boundary conditions and consider a general nonlinearity $f(\cdot) \in C^1(\mathbb{R})$, i.e.

$$u_t + \rho_x - u_{xxt} + (f(u))_x = 0, \quad (2.1a)$$

$$\rho_t + u_x = 0, \quad a < x < b, \quad t > 0, \quad (2.1b)$$

$$u(x, 0) = u_0(x), \quad \rho(x, 0) = \rho_0(x), \quad a \leq x \leq b, \quad (2.1c)$$

$$u(a, t) = u(b, t), \quad u_x(a, t) = u_x(b, t), \quad \rho(a, t) = \rho(b, t), \quad t \geq 0. \quad (2.1d)$$

With $f(u) = \frac{1}{2}u^2$, we get back the traditional SRLW equation (1.1). Noticing the periodic boundary conditions, here we first apply the Fourier spectral method for the spatial discretiza-

tions, and then design some exponential wave integrators to integrate the equations in the frequency space.

Choose mesh size $h = \Delta x = (b-a)/N$ with N a positive even integer, denote grid points as

$$x_j := a + jh, \quad j = 0, 1, \dots, N,$$

and define

$$X_N := \text{span} \left\{ \phi_l(x) = e^{i\mu_l(x-a)} : x \in \overline{\Omega}, \mu_l = \frac{2\pi l}{b-a}, l = -\frac{N}{2}, \dots, \frac{N}{2} - 1 \right\},$$

$$Y_N := \{v = (v_0, v_1, \dots, v_N) \in \mathbb{R}^{N+1} : v_0 = v_N\}.$$

For a general periodic function $v(x)$ on $\overline{\Omega} = [a, b]$ and a vector $v \in Y_N$, let $P_N : L^2(\Omega) \rightarrow X_N$ be the standard L^2 - projection operator onto X_N , $I_N : C(\Omega) \rightarrow X_N$ and $I_N : Y_N \rightarrow X_N$ be the trigonometric interpolation operator [27], i.e.

$$(P_N v)(x) = \sum_{l=-N/2}^{N/2-1} \widehat{v}_l e^{i\mu_l(x-a)}, \quad (I_N v)(x) = \sum_{l=-N/2}^{N/2-1} \widetilde{v}_l e^{i\mu_l(x-a)}, \quad a \leq x \leq b, \quad (2.2)$$

with

$$\widehat{v}_l = \frac{1}{b-a} \int_a^b v(x) e^{-i\mu_l(x-a)} dx, \quad \widetilde{v}_l = \frac{1}{N} \sum_{j=0}^{N-1} v_j e^{-i\mu_l(x_j-a)}, \quad (2.3)$$

where v_j is interpreted as $v(x_j)$. It is clear that P_N and I_N are identical operators over X_N . The Fourier spectral method [27] for spatial discretizations of equations (2.1) becomes: find $u_N(x, t)$, $\rho_N(x, t) \in X_N$, such that

$$(u_N)_t + (\rho_N)_x - (u_N)_{xxt} + P_N(f(u_N))_x = 0,$$

$$(\rho_N)_t + (u_N)_x = 0, \quad a < x < b, \quad t > 0.$$

Due to the orthogonality of the basis functions in X_N , we obtain

$$\frac{d}{dt} \widehat{u}_l(t) + i\mu_l \widehat{\rho}_l(t) + \mu_l^2 \frac{d}{dt} \widehat{u}_l(t) + i\mu_l (\widehat{f(u_N)})_l(t) = 0,$$

$$\frac{d}{dt} \widehat{\rho}_l(t) + i\mu_l \widehat{u}_l(t) = 0, \quad l = -\frac{N}{2}, \dots, \frac{N}{2} - 1, \quad t > 0.$$

Let $\tau = \Delta t > 0$ be the time step size, and denote time grids by $t_n = n\tau$ for $n = 0, 1, \dots$. Then for some $t = t_n + s$, we have

$$\frac{d}{ds} \widehat{u}_l(t_n + s) + \frac{i\mu_l}{1 + \mu_l^2} \widehat{\rho}_l(t_n + s) + \frac{i\mu_l}{1 + \mu_l^2} \widehat{f}_l^n(s) = 0, \quad (2.4a)$$

$$\frac{d}{ds} \widehat{\rho}_l(t_n + s) + i\mu_l \widehat{u}_l(t_n + s) = 0, \quad l = -\frac{N}{2}, \dots, \frac{N}{2} - 1, \quad s > 0, \quad (2.4b)$$

where we define $f^n(x, s) := f(u_N(x, t_n + s))$. The exponential wave integrators [7, 10, 20, 21] to solve the ODEs (2.4) begin with the variation-of-constant formula,

$$\widehat{u}_l(t_n + s) = \cos(\beta_l s) \widehat{u}_l(t_n) - \frac{i\beta_l}{\mu_l} \sin(\beta_l s) \widehat{\rho}_l(t_n) - \frac{i\mu_l}{1 + \mu_l^2} \int_0^s \cos(\beta_l(s - \theta)) \widehat{f}_l^n(\theta) d\theta, \quad (2.5a)$$

$$\widehat{\rho}_l(t_n + s) = -\frac{i\mu_l}{\beta_l} \sin(\beta_l s) \widehat{u}_l(t_n) + \cos(\beta_l s) \widehat{\rho}_l(t_n) - \beta_l \int_0^s \sin(\beta_l(s - \theta)) \widehat{f}_l^n(\theta) d\theta, \quad (2.5b)$$

where we denote

$$\beta_l = \frac{|\mu_l|}{\sqrt{1 + \mu_l^2}}, \quad l = -\frac{N}{2}, \dots, \frac{N}{2} - 1, \quad \text{and} \quad \frac{\beta_0}{\mu_0} := 0, \quad \frac{\mu_0}{\beta_0} := 0. \quad (2.6)$$

In order to obtain an explicit scheme, we approximate the integrals in (2.5a) by a Gautschi-type quadrature [7, 10, 20] as

$$\int_0^s \cos(\beta_l(s - \theta)) \widehat{f}_l^n(\theta) d\theta \approx \int_0^s \cos(\beta_l(s - \theta)) \left[\widehat{f}_l^n(0) + \theta \frac{d}{ds} \widehat{f}_l^n(0) \right] d\theta,$$

and then the rest parts can be integrated exactly. Applying similar quadratures to (2.5b) and then let $s = \tau$ in above, we get for $l = -\frac{N}{2}, \dots, \frac{N}{2} - 1$,

$$\begin{aligned} \widehat{u}_l(t_{n+1}) &\approx \cos(\beta_l \tau) \widehat{u}_l(t_n) - \frac{i\beta_l}{\mu_l} \sin(\beta_l \tau) \widehat{\rho}_l(t_n) \\ &\quad - \frac{i\mu_l}{1 + \mu_l^2} \left[a_l(\tau) \widehat{f}_l^n(0) + b_l(\tau) \frac{d}{ds} \widehat{f}_l^n(0) \right], \end{aligned} \quad (2.7a)$$

$$\begin{aligned} \widehat{\rho}_l(t_{n+1}) &\approx -\frac{i\mu_l}{\beta_l} \sin(\beta_l \tau) \widehat{u}_l(t_n) + \cos(\beta_l \tau) \widehat{\rho}_l(t_n) \\ &\quad - \beta_l \left[c_l(\tau) \widehat{f}_l^n(0) + d_l(\tau) \frac{d}{ds} \widehat{f}_l^n(0) \right], \end{aligned} \quad (2.7b)$$

where (the detailed formulas are given in appendix A)

$$\begin{aligned} a_l(\tau) &= \int_0^\tau \cos(\beta_l(\tau - \theta)) d\theta, \quad b_l(\tau) = \int_0^\tau \cos(\beta_l(\tau - \theta)) \cdot \theta d\theta, \\ c_l(\tau) &= \int_0^\tau \sin(\beta_l(\tau - \theta)) d\theta, \quad d_l(\tau) = \int_0^\tau \sin(\beta_l(\tau - \theta)) \cdot \theta d\theta. \end{aligned} \quad (2.8)$$

Note that

$$\frac{d}{ds} \widehat{f}_l^n(s) = \widehat{(\partial_s f^n)}_l(s) \quad \text{and} \quad \partial_s f^n(x, s) := f'(u_N(x, t_n + s)) \cdot \partial_s u_N(x, t_n + s),$$

so to complete the scheme, we need to find $\partial_s u_N(x, t_n)$ and it is directly given by (2.4a) with $s = 0$, i.e.

$$\widehat{(\partial_s u_N)}_l(t_n) = \frac{d}{ds} \widehat{u}_l(t_n) = -\frac{i\mu_l}{1 + \mu_l^2} \left[\widehat{\rho}_l(t_n) + \widehat{f}_l^n(0) \right], \quad l = -\frac{N}{2}, \dots, \frac{N}{2} - 1, \quad n = 0, 1, \dots \quad (2.9)$$

Thus, a detailed exponential wave integrator Fourier spectral (EWI-FS) method reads as follows. Let $u_N^n(x)$, $\dot{u}_N^n(x)$ and $\rho_N^n(x)$ be the approximations to $u(x, t_n)$, $\partial_t u(x, t_n)$ and $\rho(x, t_n)$, respectively. Choose $u_N^0(x) = u_0(x)$, $\rho_N^0(x) = \rho_0(x)$, then for $n = 0, 1, \dots$,

$$u_N^{n+1}(x) = \sum_{l=-N/2}^{N/2-1} \widehat{u}_l^{n+1} e^{i\mu_l(x-a)}, \quad \rho_N^{n+1}(x) = \sum_{l=-N/2}^{N/2-1} \widehat{\rho}_l^{n+1} e^{i\mu_l(x-a)}, \quad (2.10)$$

where

$$\widehat{u}_l^{n+1} = \cos(\beta_l \tau) \widehat{u}_l^n - \frac{i\beta_l}{\mu_l} \sin(\beta_l \tau) \widehat{\rho}_l^n - \frac{i\mu_l}{1 + \mu_l^2} \left[a_l(\tau) \widehat{F}_l^n + b_l(\tau) \widehat{G}_l^n \right], \quad (2.11a)$$

$$\widehat{\rho}_l^{n+1} = -\frac{i\mu_l}{\beta_l} \sin(\beta_l \tau) \widehat{u}_l^n + \cos(\beta_l \tau) \widehat{\rho}_l^n - \beta_l \left[c_l(\tau) \widehat{F}_l^n + d_l(\tau) \widehat{G}_l^n \right], \quad (2.11b)$$

with

$$F^n(x) = f(u_N^n(x)), \quad G^n(x) = f'(u_N^n(x)) \cdot \dot{u}_N^n(x), \quad (2.12a)$$

$$\dot{u}_N^n(x) = \sum_{l=-N/2}^{N/2-1} (\widehat{u})_l^n e^{i\mu_l(x-a)}, \quad (\widehat{u})_l^n = -\frac{i\mu_l}{1+\mu_l^2} [\widehat{\rho}_l^n + \widehat{F}_l^n]. \quad (2.12b)$$

In practice, the above procedure is not suitable due to the difficulty of computing the Fourier coefficients (2.11) via the integration formula given in (2.3). By approximating the integrals in (2.3) and (2.11) by a quadrature rule on the grids $\{x_j : j = 0, \dots, N\}$, we present an efficient implementation by using the interpolation stated in (2.3) rather than the projection (integration). Then an exponential wave integrator Fourier pseudospectral (EWI-FP) method reads as follows. Denote u_j^n , \dot{u}_j^n and ρ_j^n be the approximations to $u(x_j, t_n)$, $\partial_t u(x_j, t_n)$ and $\rho(x_j, t_n)$, respectively. Choose $u_j^0 = u_0(x_j)$, $\rho_j^0 = \rho_0(x_j)$ for $j = 0, 1, \dots, N$, then for $n = 0, 1, \dots$,

$$u_j^{n+1} = \sum_{l=-N/2}^{N/2-1} \widetilde{u}_l^{n+1} e^{i\mu_l(x_j-a)}, \quad \rho_j^{n+1} = \sum_{l=-N/2}^{N/2-1} \widetilde{\rho}_l^{n+1} e^{i\mu_l(x_j-a)}, \quad (2.13)$$

where

$$\widetilde{u}_l^{n+1} = \cos(\beta_l \tau) \widetilde{u}_l^n - \frac{i\beta_l}{\mu_l} \sin(\beta_l \tau) \widetilde{\rho}_l^n - \frac{i\mu_l}{1+\mu_l^2} [a_l(\tau) \widetilde{F}_l^n + b_l(\tau) \widetilde{G}_l^n], \quad (2.14a)$$

$$\widetilde{\rho}_l^{n+1} = -\frac{i\mu_l}{\beta_l} \sin(\beta_l \tau) \widetilde{u}_l^n + \cos(\beta_l \tau) \widetilde{\rho}_l^n - \beta_l [c_l(\tau) \widetilde{F}_l^n + d_l(\tau) \widetilde{G}_l^n], \quad (2.14b)$$

with

$$F_j^n = f(u_j^n), \quad G_j^n = f'(u_j^n) \cdot \dot{u}_j^n, \quad (2.15a)$$

$$\dot{u}_j^n = \sum_{l=-N/2}^{N/2-1} (\widetilde{u})_l^n e^{i\mu_l(x_j-a)}, \quad (\widetilde{u})_l^n = -\frac{i\mu_l}{1+\mu_l^2} [\widetilde{\rho}_l^n + \widetilde{F}_l^n]. \quad (2.15b)$$

The above EWI-FS (2.10)-(2.12) and EWI-FP (2.13)-(2.15) methods are fully explicit. The EWI-FP method (2.13)-(2.15) is easy to implement and very efficient due to the fast Fourier transform. The memory cost is $O(N)$ and the computational cost per time step is $O(N \log N)$. Besides, the EWI-FP method conserves the two time invariants (1.3) in a discrete level, stated as the following proposition.

Proposition 2.1. *Let u_j^n , ρ_j^n ($j = 0, 1, \dots, N, n = 0, 1, \dots$) be the numerical approximations obtained by the EWI-FP method (2.13)-(2.15), then we have the following two conservation laws in the discrete level:*

$$I_u^n := h \sum_{j=0}^{N-1} u_j^n \equiv I_u^0, \quad I_\rho^n := h \sum_{j=0}^{N-1} \rho_j^n \equiv I_\rho^0, \quad n = 0, 1, \dots \quad (2.16)$$

Proof. Noticing the fact

$$\sum_{j=0}^{N-1} e^{i\mu_l(x_j-a)} = \begin{cases} 0, & l \neq 0, \\ N, & l = 0, \end{cases} \quad (2.17)$$

thus from (2.13), we have

$$I_u^{n+1} = h \sum_{j=0}^{N-1} u_j^{n+1} = h \cdot \tilde{u}_0^{n+1}, \quad I_\rho^{n+1} = h \sum_{j=0}^{N-1} \rho_j^{n+1} = h \cdot \tilde{\rho}_0^{n+1}, \quad n = 0, 1, \dots$$

Then with $l = 0$ in (2.14) and noting (2.6), we have

$$\tilde{u}_0^{n+1} = \tilde{u}_0^n, \quad \tilde{\rho}_0^{n+1} = \tilde{\rho}_0^n,$$

which immediately imply that $I_u^{n+1} = I_u^n$, $I_\rho^{n+1} = I_\rho^n$, and the proof is completed. \square

Remark 2.1. Here we use Fourier spectral method in the case of periodic boundary conditions. We remark that corresponding sine/cosine spectral methods can be established in a similar way for homogenous Dirichlet/Neumann boundary conditions.

3. Convergence Analysis

In this section, we shall state and prove the main convergence theorem of the proposed EWI-FP method in the energy space $H^1 \times L^2$. The spectral method (2.10)-(2.12) is in fact a semi-discretization of (2.1), while the pseudospectral method (2.13)-(2.15) is a full discretization. For simplicity, here we analyze the full discretization EWI-FP method (2.13)-(2.15). The analysis for the semi-discretization case can be done in the same spirit.

3.1. Main results on the error bound in energy space

To state the main results, we introduce the periodic Sobolev space over interval $\Omega = (a, b)$ as

$$H_p^m(\Omega) = \left\{ \phi(x) \in H^m(\Omega) : \frac{d^k}{dx^k} \phi(a) = \frac{d^k}{dx^k} \phi(b), \quad k = 0, 1, \dots, m-1 \right\} \subset H^m(\Omega),$$

for some integer $m \geq 1$. In order to obtain the optimal error estimate results, we consider the sufficiently smooth initial data for the SRLW equation (2.1), and motivated from the analytical results for the SRLW equation in [11, 19], we make the following assumptions: let $0 < T \leq T^*$ with T^* the maximum existence time of the solution $u(x, t)$ and $\rho(x, t)$ to problem (2.1); assume that for some integers $m_0, k \geq 1$,

$$\begin{aligned} u &\in C([0, T]; H_p^{m_0+1} \cap L^\infty) \cap C^1([0, T]; H_p^{m_0} \cap W^{1,4}) \cap C^2([0, T]; L^2), \\ \rho &\in C([0, T]; H_p^{m_0}) \cap C^1([0, T]; L^2), \quad f \in C^{k+1}(\mathbb{R}). \end{aligned} \quad (\text{A})$$

Under assumption (A), we let

$$m := \min\{k, m_0\}, \quad K_1 := \|u\|_{L^\infty([0, T]; L^\infty(\Omega) \cap H^1(\Omega))}, \quad K_2 := \|\rho\|_{L^\infty([0, T]; L^2(\Omega))}.$$

Denote the trigonometric interpolations of numerical solutions as $u_I^n(x) := I_N(u^n)(x)$, $\rho_I^n(x) := I_N(\rho^n)(x)$, and define the ‘error’ functions as

$$e_u^n(x) := u(x, t_n) - u_I^n(x), \quad e_\rho^n(x) := \rho(x, t_n) - \rho_I^n(x), \quad x \in \Omega, \quad n \geq 0,$$

then we have the following main error estimate result:

Theorem 3.1. *Let u^n and ρ^n be the numerical approximations obtained from the EWI-FP method (2.13)-(2.15). Under the assumption (A), there exist two constants $\tau_0, h_0 > 0$, independent of τ (or n) and h , such that for any $0 < \tau < \tau_0$, $0 < h < h_0$,*

$$\|e_u^n\|_{H^1} + \|e_\rho^n\|_{L^2} \lesssim \tau^2 + h^m, \quad n = 0, 1, \dots, \frac{T}{\tau}, \quad (3.1a)$$

$$\|u_I^n\|_{H^1} \leq K_1 + 1, \quad \|\rho_I^n\|_{L^2} \leq K_2 + 1, \quad \|u^n\|_{l^\infty} \leq K_1 + 1. \quad (3.1b)$$

3.2. Proof of the main theorem

Let u, ρ be the exact solutions of the SRLW equation (2.1). Denote the L^2 -projected solutions as

$$\begin{aligned} u_N(x, t) &:= P_N(u(x, t)) = \sum_{l=-N/2}^{N/2-1} \widehat{u}_l(t) e^{i\mu_l(x-a)}, \\ \rho_N(x, t) &:= P_N(\rho(x, t)) = \sum_{l=-N/2}^{N/2-1} \widehat{\rho}_l(t) e^{i\mu_l(x-a)}, \end{aligned} \quad x \in \Omega, \quad t \geq 0,$$

and the projected error functions as

$$\begin{aligned} e_{u,N}^n(x) &:= P_N(e_u^n(x)) = \sum_{l=-N/2}^{N/2-1} (\widehat{e}_u)_l^n e^{i\mu_l(x-a)}, \\ e_{\rho,N}^n(x) &:= P_N(e_\rho^n(x)) = \sum_{l=-N/2}^{N/2-1} (\widehat{e}_\rho)_l^n e^{i\mu_l(x-a)}, \end{aligned} \quad n = 0, 1, \dots, \frac{T}{\tau}. \quad (3.2)$$

Then we should have

$$(\widehat{e}_u)_l^n = \widehat{u}_l(t_n) - \widetilde{u}_l^n, \quad (\widehat{e}_\rho)_l^n = \widehat{\rho}_l(t_n) - \widetilde{\rho}_l^n, \quad n = 0, 1, \dots, \frac{T}{\tau}. \quad (3.3)$$

Based on (2.7), define the local truncation errors for $n = 0, 1, \dots, \frac{T}{\tau} - 1$ as

$$\xi_u^n(x) := \sum_{l=-N/2}^{N/2-1} (\widehat{\xi}_u)_l^n e^{i\mu_l(x-a)}, \quad \xi_\rho^n(x) := \sum_{l=-N/2}^{N/2-1} (\widehat{\xi}_\rho)_l^n e^{i\mu_l(x-a)}, \quad x \in \Omega, \quad (3.4)$$

where

$$\begin{aligned} (\widehat{\xi}_u)_l^n &= \widehat{u}_l(t_{n+1}) - \cos(\beta_l \tau) \widehat{u}_l(t_n) + \frac{i\beta_l}{\mu_l} \sin(\beta_l \tau) \widehat{\rho}_l(t_n) + \frac{i\mu_l}{1 + \mu_l^2} \left[a_l(\tau) (\widehat{f(u)})_l(t_n) \right. \\ &\quad \left. + b_l(\tau) \frac{d}{ds} (\widehat{f(u)})_l(t_n) \right], \end{aligned} \quad (3.5a)$$

$$\begin{aligned} (\widehat{\xi}_\rho)_l^n &= \widehat{\rho}_l(t_{n+1}) + \frac{i\mu_l}{\beta_l} \sin(\beta_l \tau) \widehat{u}_l(t_n) - \cos(\beta_l \tau) \widehat{\rho}_l(t_n) + \beta_l \left[c_l(\tau) (\widehat{f(u)})_l(t_n) \right. \\ &\quad \left. + d_l(\tau) \frac{d}{ds} (\widehat{f(u)})_l(t_n) \right]. \end{aligned} \quad (3.5b)$$

Subtracting the local truncation errors (3.5) from the scheme (2.14), we are led to the error equations for $n = 0, 1, \dots, \frac{T}{\tau} - 1$ and $l = -\frac{N}{2}, \dots, \frac{N}{2} - 1$,

$$\widehat{(e_u)}_l^{n+1} = \cos(\beta_l \tau) \widehat{(e_u)}_l^n - \frac{i\beta_l}{\mu_l} \sin(\beta_l \tau) \widehat{(e_\rho)}_l^n + \widehat{(\xi_u)}_l^n - \widehat{(\eta_u)}_l^n, \quad (3.6a)$$

$$\widehat{(e_\rho)}_l^{n+1} = -\frac{i\mu_l}{\beta_l} \sin(\beta_l \tau) \widehat{(e_u)}_l^n + \cos(\beta_l \tau) \widehat{(e_\rho)}_l^n + \widehat{(\xi_\rho)}_l^n - \widehat{(\eta_\rho)}_l^n, \quad (3.6b)$$

where

$$\widehat{(\eta_u)}_l^n = \frac{i\mu_l}{1 + \mu_l^2} \left[a_l(\tau) \left(\widehat{(f(u))}_l(t_n) - \widetilde{F}_l^n \right) + b_l(\tau) \left(\frac{d}{ds} \widehat{(f(u))}_l(t_n) - \widetilde{G}_l^n \right) \right], \quad (3.7a)$$

$$\widehat{(\eta_\rho)}_l^n = \beta_l \left[c_l(\tau) \left(\widehat{(f(u))}_l(t_n) - \widetilde{F}_l^n \right) + d_l(\tau) \left(\frac{d}{ds} \widehat{(f(u))}_l(t_n) - \widetilde{G}_l^n \right) \right], \quad (3.7b)$$

with the nonlinear error functions defined as

$$\eta_u^n(x) := \sum_{l=-N/2}^{N/2-1} \widehat{(\eta_u)}_l^n e^{i\mu_l(x-a)}, \quad \eta_\rho^n(x) := \sum_{l=-N/2}^{N/2-1} \widehat{(\eta_\rho)}_l^n e^{i\mu_l(x-a)}, \quad x \in \Omega.$$

Define the error energy as

$$\mathcal{E}(P, Q) := \|P\|_{H^1}^2 + \|Q\|_{L^2}^2, \quad (3.8)$$

for two arbitrary functions $P(x)$ and $Q(x)$ on Ω .

In order to proceed to the proof of Theorem 3.1, we give the following lemmas. First of all, we have estimates for the local truncation errors, stated in the following lemma.

Lemma 3.1. *Based on assumption (A), we have estimates for the local truncation errors as*

$$\|\xi_u^n\|_{H^1} + \|\xi_\rho^n\|_{L^2} \lesssim \tau^3, \quad n = 0, 1, \dots, \frac{T}{\tau} - 1. \quad (3.9)$$

Proof. Applying the L^2 -projection on both sides of (2.1), due to the orthogonality of basis functions and the variation-of-constant formula, the Fourier coefficients $\widehat{u}_l(t_n)$ and $\widehat{\rho}_l(t_n)$ should satisfy

$$\begin{aligned} \widehat{u}_l(t_{n+1}) &= \cos(\beta_l \tau) \widehat{u}_l(t_n) - \frac{i\beta_l}{\mu_l} \sin(\beta_l \tau) \widehat{\rho}_l(t_n) \\ &\quad - \frac{i\mu_l}{1 + \mu_l^2} \int_0^\tau \cos(\beta_l(\tau - \theta)) \widehat{(f(u))}_l(t_n + \theta) d\theta, \end{aligned} \quad (3.10a)$$

$$\begin{aligned} \widehat{\rho}_l(t_{n+1}) &= -\frac{i\mu_l}{\beta_l} \sin(\beta_l \tau) \widehat{u}_l(t_n) + \cos(\beta_l \tau) \widehat{\rho}_l(t_n) \\ &\quad - \beta_l \int_0^\tau \sin(\beta_l(\tau - \theta)) \widehat{(f(u))}_l(t_n + \theta) d\theta. \end{aligned} \quad (3.10b)$$

Subtracting (3.5) from (3.10), we get

$$\begin{aligned} \widehat{(\xi_u)}_l^n &= \frac{i\mu_l}{1 + \mu_l^2} \left[a_l(\tau) \widehat{(f(u))}_l(t_n) + b_l(\tau) \frac{d}{ds} \widehat{(f(u))}_l(t_n) \right] \\ &\quad - \frac{i\mu_l}{1 + \mu_l^2} \left[\int_0^\tau \cos(\beta_l(\tau - \theta)) \widehat{(f(u))}_l(t_n + \theta) d\theta \right], \end{aligned}$$

$$\begin{aligned} \widehat{(\xi_\rho)}_l^n &= \beta_l \left[c_l(\tau) \widehat{(f(u))}_l(t_n) + d_l(\tau) \frac{d}{ds} \widehat{(f(u))}_l(t_n) \right] \\ &\quad - \beta_l \left[\int_0^\tau \sin(\beta_l(\tau - \theta)) \widehat{(f(u))}_l(t_n + \theta) d\theta \right]. \end{aligned}$$

Noting (2.8) and by the Taylor's expansion, we get

$$\begin{aligned}\widehat{(\xi_u)}_l^n &= -\frac{i\mu_l}{1+\mu_l^2} \int_0^\tau \cos(\beta_l(\tau-\theta)) \cdot \frac{\theta^2}{2} \cdot \frac{d^2}{ds^2} \widehat{(f(u))}_l(\theta^n) d\theta, \\ \widehat{(\xi_\rho)}_l^n &= -\beta_l \int_0^\tau \sin(\beta_l(\tau-\theta)) \cdot \frac{\theta^2}{2} \cdot \frac{d^2}{ds^2} \widehat{(f(u))}_l(\theta^n) d\theta,\end{aligned}$$

where $\theta^n \in [t_n, t_{n+1}]$. Then we have

$$\begin{aligned}\left| \widehat{(\xi_u)}_l^n \right| &\leq \frac{\tau^2 |\mu_l|}{2(1+\mu_l^2)} \int_0^\tau \left| \frac{d^2}{ds^2} \widehat{(f(u))}_l(\theta^n) \right| d\theta, \\ \left| \widehat{(\xi_\rho)}_l^n \right| &\leq \frac{\tau^2 \beta_l}{2} \int_0^\tau \left| \frac{d^2}{ds^2} \widehat{(f(u))}_l(\theta^n) \right| d\theta.\end{aligned}$$

Taking square on both sides of the above two inequalities, then by Hölder's inequality, we get

$$\left| \widehat{(\xi_u)}_l^n \right|^2 \lesssim \frac{\tau^5 \mu_l^2}{(1+\mu_l^2)^2} \int_0^\tau \left| \frac{d^2}{ds^2} \widehat{(f(u))}_l(\theta^n) \right|^2 d\theta, \quad (3.11a)$$

$$\left| \widehat{(\xi_\rho)}_l^n \right|^2 \lesssim \tau^5 \beta_l^2 \int_0^\tau \left| \frac{d^2}{ds^2} \widehat{(f(u))}_l(\theta^n) \right|^2 d\theta. \quad (3.11b)$$

Multiplying (3.11a) on both sides by $(1+\mu_l^2)$, then summing up for $l = -\frac{N}{2}, \dots, \frac{N}{2} - 1$ and by Parserval's identity, we get

$$\|\xi_u^n\|_{H^1}^2 \lesssim \tau^5 \int_0^\tau \|\partial_s^2 f(u(\cdot, \theta^n))\|_{L^2}^2 d\theta.$$

Under assumption (A),

$$\begin{aligned}&\int_0^\tau \|\partial_s^2 f(u(\cdot, \theta^n))\|_{L^2}^2 d\theta \\ &= \int_0^\tau \left\| f'(u(\cdot, \theta^n)) \cdot \partial_s^2 u(\cdot, \theta^n) + f''(u(\cdot, \theta^n)) \cdot (\partial_s u(\cdot, \theta^n))^2 \right\|_{L^2}^2 d\theta \lesssim \tau,\end{aligned}$$

so we get

$$\|\xi_u^n\|_{H^1}^2 \lesssim \tau^6. \quad (3.12)$$

Summing (3.11b) up for $l = -\frac{N}{2}, \dots, \frac{N}{2} - 1$ and noting (2.6), we can get

$$\|\xi_\rho^n\|_{L^2}^2 \lesssim \tau^5 \int_0^\tau \|\partial_s^2 f(u_N(\cdot, \theta^n))\|_{L^2}^2 d\theta \lesssim \tau^6. \quad (3.13)$$

Combing (3.12) and (3.13), we get assertion (3.9). \square

For the nonlinear error terms, we have estimates stated as the following lemma.

Lemma 3.2. *Based on assumption (A), and assume (3.1b) holds for some $0 \leq n \leq \frac{T}{\tau} - 1$ (which will be given by induction later), then we have*

$$\|\eta_u^n\|_{H^1} + \|\eta_\rho^n\|_{L^2} \lesssim \tau (\|e_{u,N}^n\|_{H^1} + \|e_{\rho,N}^n\|_{L^2}) + \tau \cdot h^m. \quad (3.14)$$

Proof. From (3.7), we have

$$\begin{aligned} \left| \widehat{(\eta_u)}_l^n \right| &\leq \frac{|\mu_l|}{1 + \mu_l^2} \left[|a_l(\tau)| \cdot \left| \widehat{(f(u))}_l(t_n) - \widetilde{F}_l^n \right| + |b_l(\tau)| \cdot \left| \frac{d}{ds} \widehat{(f(u))}_l(t_n) - \widetilde{G}_l^n \right| \right], \\ \left| \widehat{(\eta_\rho)}_l^n \right| &\leq \beta_l \left[|c_l(\tau)| \cdot \left| \widehat{(f(u))}_l(t_n) - \widetilde{F}_l^n \right| + |d_l(\tau)| \cdot \left| \frac{d}{ds} \widehat{(f(u))}_l(t_n) - \widetilde{G}_l^n \right| \right], \end{aligned}$$

Noticing from (2.8) that

$$|a_l(\tau)|, |b_l(\tau)|, |c_l(\tau)|, |d_l(\tau)| \lesssim \tau, \quad l = -\frac{N}{2}, \dots, \frac{N}{2} - 1,$$

then similarly as before, we can get

$$\|\eta_u^n\|_{H^1}^2 \lesssim \tau^2 \left[\|P_N f(u(\cdot, t_n)) - I_N F^n\|_{L^2}^2 + \|P_N \partial_t f(u(\cdot, t_n)) - I_N G^n\|_{L^2}^2 \right], \quad (3.15a)$$

$$\|\eta_\rho^n\|_{L^2}^2 \lesssim \tau^2 \left[\|P_N f(u(\cdot, t_n)) - I_N F^n\|_{L^2}^2 + \|P_N \partial_t f(u(\cdot, t_n)) - I_N G^n\|_{L^2}^2 \right]. \quad (3.15b)$$

By the standard interpolation error bound [27] together with assumption (A) and Parserval's identity, we find

$$\begin{aligned} &\|P_N f(u(\cdot, t_n)) - I_N F^n\|_{L^2} \\ &\leq \|I_N f(u(\cdot, t_n)) - I_N F^n\|_{L^2} + \|P_N f(u(\cdot, t_n)) - I_N f(u)(\cdot, t_n)\|_{L^2} \\ &\lesssim \|f(u(\cdot, t_n)) - f(u^n)\|_{l^2} + h^m. \end{aligned} \quad (3.16)$$

Meanwhile, we also have

$$\|P_N \partial_t f(u(\cdot, t_n)) - I_N G^n\|_{L^2} \lesssim \|f'(u(\cdot, t_n)) \cdot \partial_t u(\cdot, t_n) - f'(u^n) \cdot \dot{u}^n\|_{l^2} + h^m. \quad (3.17)$$

With the induction assumption (3.1b), we have

$$\begin{aligned} \|f(u(\cdot, t_n)) - f(u^n)\|_{l^2} &= \left\| \int_0^1 f'(\omega u(\cdot, t_n) + (1 - \omega)u^n) d\omega \cdot (u(\cdot, t_n) - u^n) \right\|_{l^2} \\ &\lesssim \|u(\cdot, t_n) - u^n\|_{l^2} \lesssim \|e_u^n\|_{L^2}, \end{aligned}$$

which together with (3.16) lead to

$$\|P_N f(u(\cdot, t_n)) - I_N F^n\|_{L^2} \lesssim \|e_u^n\|_{L^2} + h^m, \quad (3.18)$$

and we have

$$\begin{aligned} &\|f'(u(\cdot, t_n)) \cdot \partial_t u(\cdot, t_n) - f'(u^n) \cdot \dot{u}^n\|_{l^2} \\ &\lesssim \|(f'(u(\cdot, t_n)) - f'(u^n)) \cdot \partial_t u(\cdot, t_n)\|_{l^2} + \|f'(u^n) \cdot (\partial_t u(\cdot, t_n) - \dot{u}^n)\|_{l^2} \\ &\lesssim \|f'(u(\cdot, t_n)) - f'(u^n)\|_{l^2} + \|\partial_t u(\cdot, t_n) - \dot{u}^n\|_{l^2} \\ &\lesssim \|e_u^n\|_{L^2} + \|\partial_t u(\cdot, t_n) - \dot{u}^n\|_{l^2}. \end{aligned} \quad (3.19)$$

For the last part in (3.19), by Parserval's identity and the interpolation error, we have

$$\begin{aligned} \|\partial_t u(\cdot, t_n) - \dot{u}^n\|_{l^2}^2 &\lesssim \|I_N \partial_t u(\cdot, t_n) - I_N \dot{u}^n\|_{L^2}^2 \\ &\lesssim \|P_N \partial_t u(\cdot, t_n) - I_N \dot{u}^n\|_{L^2}^2 + h^{2m} = \sum_{l=-\frac{N}{2}}^{\frac{N}{2}-1} \left| \frac{d}{ds} \widehat{u}_l(t_n) - \widehat{(\dot{u})}_l^n \right|^2 + h^{2m}. \end{aligned} \quad (3.20)$$

Noting from (2.1a), we have

$$\frac{d}{ds}\widehat{u}_l(t_n) = -\frac{i\mu_l}{1+\mu_l^2} \left[\widehat{\rho}_l(t_n) + \widehat{(f(u))}_l(t_n) \right], \quad l = -\frac{N}{2}, \dots, \frac{N}{2} - 1. \quad (3.21)$$

Then subtracting (3.21) from (2.15b), we get

$$\left| \frac{d}{ds}\widehat{u}_l(t_n) - \widehat{(u)}_l^n \right| \lesssim |\widehat{\rho}_l(t_n) - \widetilde{\rho}_l^n| + \left| \widehat{(f(u))}_l(t_n) - \widetilde{F}_l^n \right|, \quad l = -\frac{N}{2}, \dots, \frac{N}{2} - 1. \quad (3.22)$$

Plugging (3.22) back to (3.20), we get

$$\begin{aligned} \|\partial_t u(\cdot, t_n) - \dot{u}^n\|_{l^2}^2 &\lesssim h^{2m} + \sum_{l=-\frac{N}{2}}^{\frac{N}{2}-1} |\widehat{\rho}_l(t_n) - \widetilde{\rho}_l^n|^2 + \left| \widehat{(f(u))}_l(t_n) - \widetilde{F}_l^n \right|^2 \\ &\lesssim \|e_{\rho, N}^n\|_{L^2}^2 + \|P_N f(u(\cdot, t_n)) - I_N F^n\|_{L^2}^2 + h^{2m} \\ &\lesssim \|e_{\rho, N}^n\|_{L^2}^2 + \|e_u^n\|_{L^2}^2 + h^{2m}. \end{aligned} \quad (3.23)$$

Then plugging (3.23) back to (3.19), we get

$$\|f'(u(\cdot, t_n)) \cdot \partial_t u(\cdot, t_n) - f'(u^n) \cdot \dot{u}^n\|_{l^2} \lesssim \|e_{\rho, N}^n\|_{L^2} + \|e_u^n\|_{L^2} + h^m,$$

which together with (3.17) lead to

$$\|P_N \partial_t f(u)(\cdot, t_n) - I_N G^n\|_{L^2} \lesssim \|e_{\rho, N}^n\|_{L^2} + \|e_u^n\|_{L^2} + h^m. \quad (3.24)$$

In addition, by the projection error estimate, we have

$$\|e_u^n\|_{L^2} \leq \|u(\cdot, t_n) - P_N u(\cdot, t_n)\|_{L^2} + \|e_{u, N}^n\| \lesssim \|e_{u, N}^n\| + h^m,$$

thus (3.18) and (3.24) become

$$\|P_N f(u(\cdot, t_n)) - I_N F^n\|_{L^2} \lesssim \|e_{u, N}^n\|_{L^2} + h^m, \quad (3.25a)$$

$$\|P_N \partial_t f(u)(\cdot, t_n) - I_N G^n\|_{L^2} \lesssim \|e_{\rho, N}^n\|_{L^2} + \|e_{u, N}^n\|_{L^2} + h^m. \quad (3.25b)$$

Finally, plugging (3.25) back to (3.15), we get assertion (3.14). \square

With the error energy functional notation (3.8), it is ready to show the following fact.

Lemma 3.3. *For $n = 0, 1, \dots, \frac{T}{\tau} - 1$, we have*

$$\mathcal{E}(e_{u, N}^{n+1}, e_{\rho, N}^{n+1}) - \mathcal{E}(e_{u, N}^n, e_{\rho, N}^n) \lesssim \tau \mathcal{E}(e_{u, N}^n, e_{\rho, N}^n) + \frac{1}{\tau} [\mathcal{E}(\xi_u^n, \xi_\rho^n) + \mathcal{E}(\eta_u^n, \eta_\rho^n)]. \quad (3.26)$$

Proof. From (3.6), we have

$$\begin{aligned} \left| \widehat{(e_u)}_l^{n+1} \right| &\leq \left| \cos(\beta_l \tau) \widehat{(e_u)}_l^n - \frac{i\beta_l}{\mu_l} \sin(\beta_l \tau) \widehat{(e_\rho)}_l^n \right| + \left| \widehat{(\xi_u)}_l^n - \widehat{(\eta_u)}_l^n \right|, \\ \left| \widehat{(e_\rho)}_l^{n+1} \right| &\leq \left| -\frac{i\mu_l}{\beta_l} \sin(\beta_l \tau) \widehat{(e_u)}_l^n + \cos(\beta_l \tau) \widehat{(e_\rho)}_l^n \right| + \left| \widehat{(\xi_\rho)}_l^n - \widehat{(\eta_\rho)}_l^n \right|. \end{aligned}$$

Taking square on both sides of the above two inequalities, and then by the Cauchy's inequality, we get

$$\begin{aligned} \left| \widehat{(e_u)}_l^{n+1} \right|^2 &\leq (1 + \tau) \left| \cos(\beta_l \tau) \widehat{(e_u)}_l^n - \frac{i\beta_l}{\mu_l} \sin(\beta_l \tau) \widehat{(e_\rho)}_l^n \right|^2 \\ &\quad + \left(1 + \frac{1}{\tau} \right) \left| \widehat{(\xi_u)}_l^n - \widehat{(\eta_u)}_l^n \right|^2, \end{aligned} \quad (3.27a)$$

$$\begin{aligned} \left| \widehat{(e_\rho)}_l^{n+1} \right|^2 &\leq (1 + \tau) \left| -\frac{i\mu_l}{\beta_l} \sin(\beta_l \tau) \widehat{(e_u)}_l^n + \cos(\beta_l \tau) \widehat{(e_\rho)}_l^n \right|^2 \\ &\quad + \left(1 + \frac{1}{\tau} \right) \left| \widehat{(\xi_\rho)}_l^n - \widehat{(\eta_\rho)}_l^n \right|^2. \end{aligned} \quad (3.27b)$$

Multiplying (3.27a) by $(1 + \mu_l^2)$ on both sides and then adding to (3.27b), noting the fact

$$\begin{aligned} &(1 + \mu_l^2) \left| \cos(\beta_l \tau) \widehat{(e_u)}_l^n - \frac{i\beta_l}{\mu_l} \sin(\beta_l \tau) \widehat{(e_\rho)}_l^n \right|^2 \\ &\quad + \left| -\frac{i\mu_l}{\beta_l} \sin(\beta_l \tau) \widehat{(e_u)}_l^n + \cos(\beta_l \tau) \widehat{(e_\rho)}_l^n \right|^2 \\ &= (1 + \mu_l^2) \left| \widehat{(e_u)}_l^n \right|^2 + \left| \widehat{(e_\rho)}_l^n \right|^2, \quad l = -\frac{N}{2}, \dots, \frac{N}{2} - 1, \end{aligned}$$

we get

$$\begin{aligned} &(1 + \mu_l^2) \left| \widehat{(e_u)}_l^{n+1} \right|^2 + \left| \widehat{(e_\rho)}_l^{n+1} \right|^2 \\ &\leq (1 + \tau) \left[(1 + \mu_l^2) \left| \widehat{(e_u)}_l^n \right|^2 + \left| \widehat{(e_\rho)}_l^n \right|^2 \right] \\ &\quad + \left(1 + \frac{1}{\tau} \right) \left[(1 + \mu_l^2) \left| \widehat{(\xi_u)}_l^n - \widehat{(\eta_u)}_l^n \right|^2 + \left| \widehat{(\xi_\rho)}_l^n - \widehat{(\eta_\rho)}_l^n \right|^2 \right]. \end{aligned} \quad (3.28)$$

Summing the inequality (3.28) up for $l = -\frac{N}{2}, \dots, \frac{N}{2} - 1$, then from (3.8) by Parseval's identity and Cauchy's inequality, we get

$$\begin{aligned} \mathcal{E}(e_{u,N}^{n+1}, e_{\rho,N}^{n+1}) - \mathcal{E}(e_{u,N}^n, e_{\rho,N}^n) &\leq \tau \mathcal{E}(e_{u,N}^n, e_{\rho,N}^n) + \left(1 + \frac{1}{\tau} \right) \mathcal{E}(\xi_u^n - \eta_u^n, \xi_\rho^n - \eta_\rho^n) \\ &\lesssim \tau \mathcal{E}(e_{u,N}^n, e_{\rho,N}^n) + \frac{1}{\tau} [\mathcal{E}(\xi_u^n, \xi_\rho^n) + \mathcal{E}(\eta_u^n, \eta_\rho^n)]. \quad \square \end{aligned}$$

Now, combining the Lemma 3.1-3.3, we give the proof of Theorem 3.1 with the help of mathematical induction argument [8, 16], or the equivalent cut-off technique [5, 30] for the boundedness of numerical solutions.

Proof of Theorem 3.1. For $n = 0$, from the scheme and assumption (A), we have

$$\|e_u^0\|_{H^1} + \|e_\rho^0\|_{L^2} = \|u_0 - I_N u_0\|_{H^1} + \|\rho_0 - I_N \rho_0\|_{L^2} \lesssim h^m.$$

Then by triangle inequality,

$$\|u_I^0\|_{H^1} \leq \|u_0\|_{H^1} + \|e_u^0\|_{H^1} \leq K_1 + 1, \quad \|\rho_I^0\|_{L^2} \leq \|\rho_0\|_{L^2} + \|e_\rho^0\|_{L^2} \leq K_2 + 1,$$

for $0 < h \leq h_1$, where $h_1 > 0$ is a constant independent of h and τ , and obviously $\|u^0\|_{l^\infty} \leq K_1 + 1$. Thus, (3.1) is true for $n = 0$.

Assume (3.1) is valid for $n \leq M \leq T/\Delta t - 1$. Now we need to show the results still hold for $n = M + 1$. First of all, by triangle inequality and projection error estimate with assumption (A),

$$\begin{aligned} & \|e_u^{M+1}\|_{H^1} + \|e_\rho^{M+1}\|_{L^2} \\ & \leq \|e_{u,N}^{M+1}\|_{H^1} + \|e_{\rho,N}^{M+1}\|_{L^2} + \|u(\cdot, t_{M+1}) - u_N(\cdot, t_{M+1})\|_{H^1} \\ & \quad + \|\rho(\cdot, t_{M+1}) - \rho_N(\cdot, t_{M+1})\|_{L^2} \\ & \lesssim \|e_{u,N}^{M+1}\|_{H^1} + \|e_{\rho,N}^{M+1}\|_{L^2} + h^m. \end{aligned} \quad (3.29)$$

Since (3.1b) is assumed to be true under induction for all $n \leq N$, so we can plug the estimates (3.9) from Lemma 3.1 and (3.14) from Lemma 3.2 into (3.26) and get

$$\mathcal{E}(e_{u,N}^{n+1}, e_{\rho,N}^{n+1}) - \mathcal{E}(e_{u,N}^n, e_{\rho,N}^n) \lesssim \tau \mathcal{E}(e_{u,N}^n, e_{\rho,N}^n) + \tau^5 + \tau \cdot h^{2m}. \quad (3.30)$$

Summing (3.30) up for $n = 0, 1, \dots, M$, and then by the discrete Gronwall's inequality, we get

$$\mathcal{E}(e_{u,N}^{M+1}, e_{\rho,N}^{M+1}) \lesssim \tau^4 + h^{2m}.$$

Thus, we have $\|e_{u,N}^{M+1}\|_{H^1} + \|e_{\rho,N}^{M+1}\|_{L^2} \leq \tau^2 + h^m$, which together with (3.29) show that (3.1b) is valid for $n = M + 1$. Then by triangle inequality,

$$\begin{aligned} \|u_I^{M+1}\|_{H^1} & \leq \|u(\cdot, t_{M+1})\|_{H^1} + \|e_u^{M+1}\|_{H^1} \leq K_1 + 1, \\ \|\rho_I^{M+1}\|_{L^2} & \leq \|\rho(\cdot, t_{M+1})\|_{L^2} + \|e_\rho^{M+1}\|_{L^2} \leq K_2 + 1, \end{aligned} \quad 0 < \tau \leq \tau_1, \quad 0 < h \leq h_2,$$

for some constants $\tau_1, h_2 > 0$ independent of τ and h . Noting the Sobolev's inequality

$$\|e_u^{M+1}\|_{L^\infty} \lesssim \|e_u^{M+1}\|_{H^1},$$

we also have

$$\|u^{M+1}\|_{l^\infty} \leq \|u_I^{M+1}\|_{L^\infty} \leq \|u(\cdot, t_{M+1})\|_{L^\infty} + \|e_u^{M+1}\|_{L^\infty} \leq K_1 + 1,$$

for $0 < \tau \leq \tau_2, 0 < h \leq h_3$, where $\tau_2, h_3 > 0$ are two constants independent of τ and h . Therefore, the proof is completed by choosing $\tau_0 = \min\{\tau_1, \tau_2\}$ and $h_0 = \min\{h_1, h_2, h_3\}$. \square

Remark 3.1. For smooth solution of the SRLW equation, we have the spectral accuracy in the space approximation from the error bound (3.1a). However for solution with less regularity, e.g. $m = 1$ or $m = 2$, the spatial convergence rate will drop down to 1st or 2nd order in h , which is similar to the classical finite difference discretization.

Remark 3.2. The two constants τ_0 and h_0 given in Theorem 3.1 essentially depend on the norms of the solutions, the nonlinearity and the physical time T , but they are totally independent of the time step τ and mesh size h . Thus, the error bounds are satisfied under no CFL-type conditions.

Remark 3.3. By the convergence theorem, we claim that no CFL-type condition is not needed for the proposed EWI-FP method. Note that the usual CFL condition refers to the constraint on time step and mesh size to guarantee the absolute stability or strong stability of numerical methods [24], which can only be obtained by the linear or von Neumann stability analysis. Here the CFL-type constraint we are referring to is the condition required by the finite time error estimate to provide the finite time convergence of numerical methods, i.e. the practical stability condition [24]. We do not claim the proposed EWI-FP is absolutely stable without any conditions theoretically, though numerically it appears to be as shall be seen in the next section.

4. Numerical Results

In this section, we shall test the proposed EWI-FP method (2.13)-(2.15) and report the numerical results to confirm the theoretical results.

We test the numerical method with two different nonlinearities: one is the classical quadratic function, the other is a general nonlinearity. For the computations, we truncate the problem onto the finite domain $\Omega = [-25, 25]$, i.e. $b = -a = 25$ in (2.1), which is large enough such that the periodic boundary conditions (2.1d) do not introduce significant aliasing errors relative to the whole space problem during the computing. To qualify the error, we use the standard H^1 -norm for variable u and L^2 -norm for variable ρ , i.e. exactly the same as the error forms given in Theorem 3.1.

4.1. Classical nonlinearity

Take the nonlinearity in the SRLW equation (2.1) as

$$f(u) = \frac{1}{2}u^2,$$

i.e. the standard SRLW (1.1). We test the accuracy of the numerical method by using two different kinds of initial data: one is the soliton inputs (1.4), the other is some general inputs.

Soliton inputs

Taking initial conditions in (2.1c) as the soliton (1.4) at $t = 0$, i.e.

$$\begin{aligned} u_0(x) &= u_S(x, t = 0; v, x_0) = \frac{3(v^2 - 1)}{v} \operatorname{sech}^2 \left(\sqrt{\frac{v^2 - 1}{4v^2}} x + x_0 \right), \\ \rho_0(x) &= \rho_S(x, t = 0; v, x_0) = \frac{3(v^2 - 1)}{v^2} \operatorname{sech}^2 \left(\sqrt{\frac{v^2 - 1}{4v^2}} x + x_0 \right), \quad x \in \Omega, \end{aligned}$$

and choosing $v = 2$ and $x_0 = 5$, we solve the SRLW equation (2.1) numerically by the EWI-FP (2.13)-(2.15) till $t = 10$. We test the spatial and temporal discretization errors separately. Firstly, for the discretization error in space, we take a very small time step $\tau = 10^{-5}$ such that the error from the discretization in time is negligible compared to the spatial discretization error. The errors are presented at $t = 5$ and tabulated in Table 4.1. Secondly, for the discretization error in time, we take a fine mesh size $h = 1/8$ such that the error from the discretization in space is negligible compared to the temporal discretization error. The errors are presented at $t = 5$ as well and tabulated in Table 4.2. To study the stability issue of the EWI-FP, Table 4.3 shows the error $\|e_u^n\|_{H^1} + \|e_\rho^n\|_{L^2}$ at some time t under several large time steps τ and very small mesh size h . The profile of the solitons during the computation till $t = 15$ are plotted in Fig. 4.1. We remark that when the soliton hits the boundary in the computation, due to the periodic boundary conditions, it will enter the domain immediately from the other side of the boundary and move on.

We then take the sum of two well-separated solitons as initial data

$$\begin{aligned} u_0(x) &= u_S(x, 0; v_1, x_1) + u_S(x, 0; v_2, x_2), \\ \rho_0(x) &= \rho_S(x, 0; v_1, x_1) + \rho_S(x, 0; v_2, x_2), \quad x \in \Omega, \end{aligned} \tag{4.1}$$

and study the dynamics of the solitons in the SRLW equation with $x_1 = -x_2 = 8, v_1 = -v_2 = 2$ for head-on collisions and $x_1 = 8, x_2 = 19, v_1 = 2, v_2 = 4.5$ for catch-up collisions of the solitons.

Table 4.1: Spatial error analysis of EWI-FP for different h at time $t = 5$ under $\tau = 10^{-5}$ with soliton inputs and classical nonlinearity.

| EWI-FP | $h_0 = 2$ | $h_0/2$ | $h_0/4$ | $h_0/8$ | $h_0/16$ |
|----------------------|-----------|----------|----------|----------|----------|
| $\ e_u^n\ _{H^1}$ | 6.82E-02 | 8.70E-04 | 3.60E-08 | 5.45E-10 | 2.54E-10 |
| $\ e_\rho^n\ _{L^2}$ | 4.91E-01 | 9.00E-03 | 2.55E-07 | 1.42E-09 | 1.01E-09 |

Table 4.2: Temporal error analysis of EWI-FP for different τ at time $t = 5$ under $h = 1/8$ with soliton inputs and classical nonlinearity.

| EWI-FP | $\tau_0 = 0.2$ | $\tau_0/2$ | $\tau_0/4$ | $\tau_0/8$ | $\tau_0/16$ |
|----------------------|----------------|------------|------------|------------|-------------|
| $\ e_u^n\ _{H^1}$ | 5.61E-02 | 1.30E-02 | 3.10E-03 | 7.72E-04 | 1.92E-04 |
| $\ e_\rho^n\ _{L^2}$ | 6.81E-02 | 1.62E-02 | 4.00E-03 | 9.83E-04 | 2.44E-04 |

Table 4.3: Stability study of EWI-FP: $\|e_u^n\|_{H^1} + \|e_\rho^n\|_{L^2}$ at $t = 5$ and $t = 10$ under some large τ and very small h for the classical nonlinearity and soliton solution case.

| $h = 1/2^9$ | $\tau_0 = 0.2$ | $\tau_0/2$ | $\tau_0/4$ |
|----------------|----------------|------------|------------|
| $t = 5$ | 7.20E-02 | 1.67E-02 | 4.00E-03 |
| $t = 10$ | 1.48E-01 | 3.18E-02 | 1.39E-02 |
| $h = 1/2^{10}$ | $\tau_0 = 0.2$ | $\tau_0/2$ | $\tau_0/4$ |
| $t = 5$ | 6.96E-02 | 1.61E-02 | 3.90E-03 |
| $t = 10$ | 1.44E-01 | 3.31E-02 | 1.81E-02 |

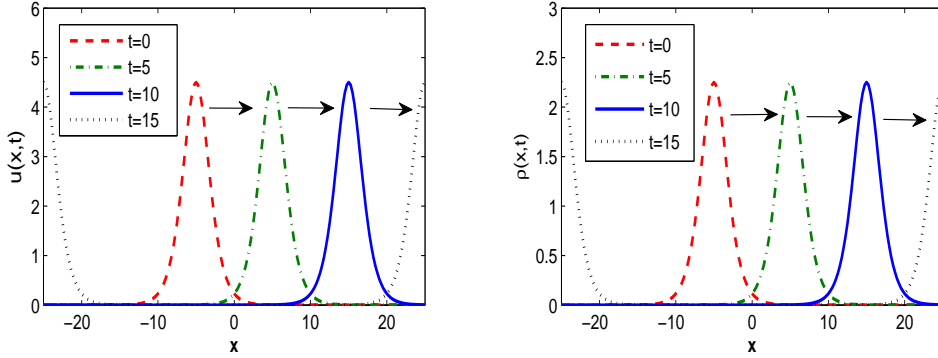


Fig. 4.1. Profile of the solitons during computing with $\tau = 0.01$ and $h = 1/8$: the left one is for $u(x, t)$ and the right one is for $\rho(x, t)$.

General inputs

To guarantee different frequencies are presented in the solution, we now choose some general initial conditions in (2.1c) as

$$u_0(x) = \frac{3 \sin(x)}{e^{0.5x^2} + e^{-0.5x^2}}, \quad \rho_0(x) = \frac{2e^{-x^2}}{\sqrt{\pi}}, \quad x \in \Omega. \quad (4.2)$$

The spatial error and temporal error are shown in Table 4.4 and Table 4.5, respectively. In this case, the ‘exact’ solution is obtained numerically by EWI-FP with very fine mesh size and

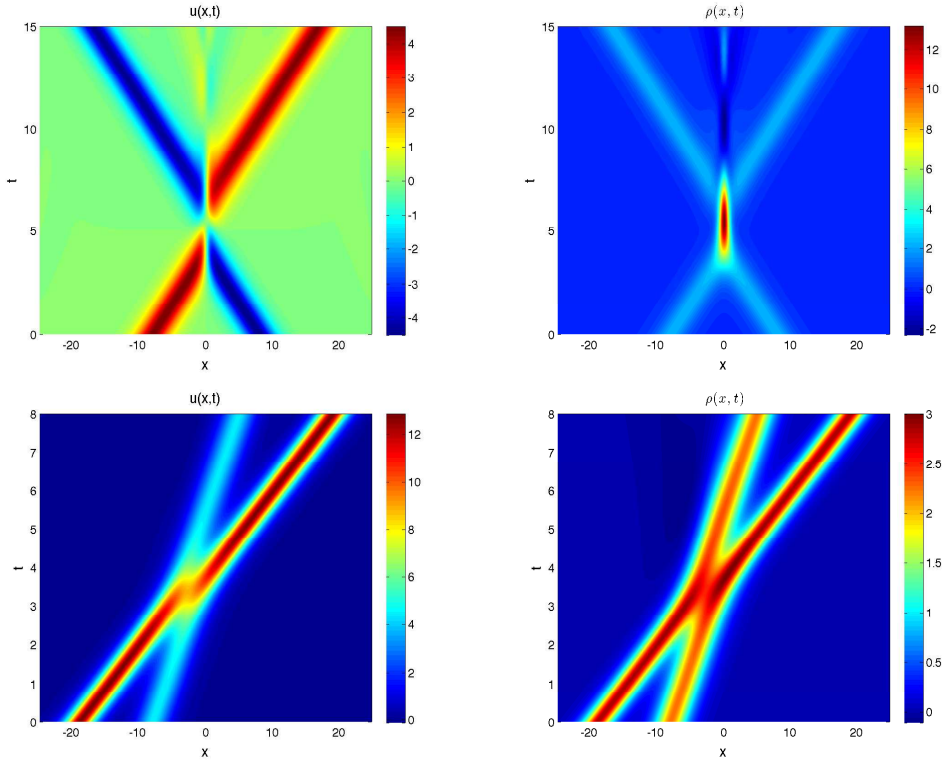


Fig. 4.2. Head-on and catch-up collisions of the solitons (4.1).

Table 4.4: Spatial error analysis of EWI-FP for different h at time $t = 5$ under $\tau = 10^{-5}$ with general inputs and classical nonlinearity.

| EWI-FP | $h_0 = 1$ | $h_0/2$ | $h_0/4$ | $h_0/8$ | $h_0/16$ |
|----------------------|-----------|----------|----------|----------|----------|
| $\ e_u^n\ _{H^1}$ | 7.80E-03 | 3.02E-04 | 1.52E-07 | 3.77E-14 | 1.35E-15 |
| $\ e_\rho^n\ _{L^2}$ | 5.53E-01 | 2.01E-02 | 4.49E-06 | 9.15E-13 | 8.28E-15 |

Table 4.5: Temporal error analysis of EWI-FP for different τ at time $t = 5$ under $h = 1/8$ with general inputs and classical nonlinearity.

| EWI-FP | $\tau_0 = 0.2$ | $\tau_0/2$ | $\tau_0/4$ | $\tau_0/8$ | $\tau_0/16$ |
|----------------------|----------------|------------|------------|------------|-------------|
| $\ e_u^n\ _{H^1}$ | 4.87E-04 | 1.19E-04 | 2.94E-05 | 7.32E-06 | 1.82E-06 |
| $\ e_\rho^n\ _{L^2}$ | 1.80E-03 | 4.46E-04 | 1.11E-04 | 2.79E-05 | 6.96E-06 |

small time step, e.g. $h = 1/16$ and $\tau = 10^{-5}$.

4.2. General nonlinearity

Now to convince our scheme works for the general nonlinearity case, we take in the SRLW equation (2.1)

$$f(u) = 5 \sin(u),$$

Table 4.6: Spatial error analysis of EWI-FP for different h at time $t = 5$ under $\tau = 10^{-5}$ with general nonlinearity.

| EWI-FP | $h_0 = 1$ | $h_0/2$ | $h_0/4$ | $h_0/8$ | $h_0/16$ |
|----------------------|-----------|----------|----------|----------|-----------|
| $\ e_u^n\ _{H^1}$ | 5.43E-02 | 2.00E-03 | 1.11E-05 | 1.00E-10 | 1.23E-015 |
| $\ e_\rho^n\ _{L^2}$ | 4.60E-01 | 2.64E-02 | 3.69E-05 | 1.03E-10 | 8.27E-015 |

Table 4.7: Temporal error analysis of EWI-FP for different τ at time $t = 5$ under $h = 1/8$ with general nonlinearity.

| EWI-FP | $\tau_0 = 0.2$ | $\tau_0/2$ | $\tau_0/4$ | $\tau_0/8$ | $\tau_0/16$ |
|----------------------|----------------|------------|------------|------------|-------------|
| $\ e_u^n\ _{H^1}$ | 8.71E-02 | 2.33E-02 | 6.10E-03 | 1.60E-03 | 3.96E-04 |
| $\ e_\rho^n\ _{L^2}$ | 7.68E-02 | 2.01E-02 | 5.20E-03 | 1.30E-03 | 3.35E-04 |

Table 4.8: Stability study of EWI-FP: $\|e_u^n\|_{H^1} + \|e_\rho^n\|_{L^2}$ at $t = 5$ and $t = 10$ under some large τ and small h for the general nonlinearity and initial data case.

| $h = 1/2^9$ | $\tau_0 = 0.2$ | $\tau_0/2$ | $\tau_0/4$ |
|----------------|----------------|------------|------------|
| $t = 5$ | 1.28E-01 | 4.06E-02 | 1.06E-02 |
| $t = 10$ | 3.01E-01 | 8.08E-02 | 2.14E-02 |
| $h = 1/2^{10}$ | $\tau_0 = 0.2$ | $\tau_0/2$ | $\tau_0/4$ |
| $t = 5$ | 1.53E-01 | 4.06E-02 | 1.06E-03 |
| $t = 10$ | 3.01E-01 | 8.08E-02 | 2.14E-02 |

and choose the initial data same as (4.2). The corresponding numerical results are shown in Tables 4.6-4.7 for spatial and temporal discretization error. Table 4.8 studies the stability of the EWI-FP method similarly as before in this case. The dynamics of the solution are shown in Fig. 4.3

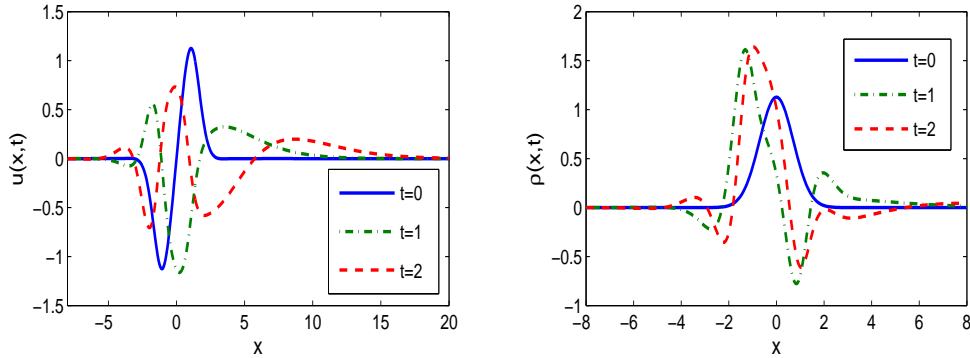


Fig. 4.3. Dynamics of the solution of the SRLW equation in the general nonlinear case.

From Tables 4.1-4.8, Figs. 4.1-4.3 and additional results not shown here brevity, we can draw the following observations:

1. The EWI-FP method (2.13)-(2.15) is of spectral accuracy in space (cf. Tables 4.1 & 4.4 &

- 4.6), and is of second-order accuracy in time (cf. Tables 4.2 & 4.5 & 4.7), which confirms the theoretical error estimates (3.1a) and indicates the results there are optimal.
2. The EWI-FP method is very stable and allows to use large time step and mesh size which are free from any CFL-type conditions (cf. Tables 4.3 & 4.8).
 3. Furthermore, the method is very efficient and low in memory cost for computing thanks to the fast Fourier transform.
 4. The EWI-FP method could simulate the dynamics of the SRLW equation accurately (cf. Figs. 4.1-4.3). The soliton is very stable. Extra waves will generate after the collision of two solitons (cf. Fig. 4.2) which indicates that the interaction between solitons is not elastic and the SRLW equation is not integrable.

5. Conclusion

In this work, a very efficient and accurate exponential wave integrator Fourier pseudospectral (EWI-FP) method was proposed and analyzed for solving the symmetric regularized-long-wave (SRLW) equation, which is used for modeling the weakly nonlinear ion acoustic and space-charge waves. The numerical method here is by applying the Fourier pseudospectral method for spatial discretization at first, and then using a Gautschi-type exponential wave integrator to integrate the differential equations in frequency space. The scheme is fully explicit and very efficient due to the fast Fourier transform. Numerical analysis of the proposed EWI-FP method was carried out and rigorous error estimate results were established without CFL-type condition by means of the mathematical induction (or cut-off technique). The error bound shows that the EWI-FP method has second order accuracy in time and spectral accuracy in space. Extensive numerical experiments were done and reported to confirm the theoretical results and show that the error bound here is optimal.

A. Detailed Formulas of the Integration Coefficients (2.8)

Here we give the detailed formulas of the integration coefficients (2.8) used in the EWI-FS (2.11) and EWI-FP (2.14). For $l = -\frac{N}{2}, \dots, \frac{N}{2} - 1$,

$$a_l(\tau) = \begin{cases} \frac{\sin(\beta_l \tau)}{\beta_l}, & l \neq 0, \\ \tau, & l = 0, \end{cases} \quad b_l(\tau) = \begin{cases} \frac{1 - \cos(\beta_l \tau)}{\beta_l^2}, & l \neq 0, \\ \frac{\tau^2}{2}, & l = 0, \end{cases} \quad (\text{A.1})$$

$$c_l(\tau) = \begin{cases} \frac{1 - \cos(\beta_l \tau)}{\beta_l}, & l \neq 0, \\ 0, & l = 0, \end{cases} \quad d_l(\tau) = \begin{cases} \frac{\beta_l \tau - \sin(\beta_l \tau)}{\beta_l^2}, & l \neq 0, \\ 0, & l = 0. \end{cases} \quad (\text{A.2})$$

Acknowledgments. The author would like to thank the editor for the kind help and the referees for their very useful suggestions.

References

- [1] F. Abdullaev, S. Darmanyan and P. Khabibullaev, *Optical Solitons*, Springer, New York, 1993.
- [2] M.J. Ablowitz and H. Segur, *Solitons and the Inverse Scattering Transform*, SIAM, Philadelphia, 1981.
- [3] J. Albert, On the decay of solutions of the generalized Benjamin-Bona-Mahony equations, *J. Math. Anal. Appl.*, **141** (1989), 527-537.
- [4] C.J. Amick, J.L. Bona and M.E. Schonbek, Decay of solutions of some nonlinear wave equations, *J. Differential Equations*, **81** (1989), 1-49.
- [5] W. Bao and Y. Cai, Optimal error estimates of finite difference methods for the Gross-Pitaevskii equation with angular momentum rotation, *Math. Comp.*, **82** (2013), 99-128.
- [6] W. Bao and Y. Cai, Uniform and optimal error estimates of an exponential wave integrator sine pseudospectral method for the nonlinear Schrödinger equation with wave operator, *SIAM J. Numer. Anal.*, **52** (2014), 1103-1127.
- [7] W. Bao, Y. Cai and X. Zhao, A uniformly correct multiscale time integrator pseudospectral method for Klein-Gordon equation in the nonrelativistic limit regime, *SIAM J. Numer. Anal.*, **52** (2014), 2488-2511.
- [8] W. Bao and X. Dong, Analysis and comparison of numerical methods for Klein-Gordon equation in nonrelativistic limit regime, *Numer. Math.*, **120** (2012), 189-229.
- [9] W. Bao, X. Dong and X. Zhao, An exponential wave integrator sine pseudospectral method for the Klein-Gordon-Zakharov system, *SIAM J. Sci. Comput.*, **25** (2013), A2903-A2927.
- [10] W. Bao, X. Dong and X. Zhao, Uniformly correct multiscale time integrators for highly oscillatory second order differential equations, *J. Math. Study*, **47** (2014), 111-150.
- [11] C.B. Brango, The Symmetric Regularized-Long-Wave equation: Well-posedness and nonlinear stability, *Phys. D*, **241** (2012), 125-133.
- [12] I.L. Bogolubsky, Some examples of inelastic soliton interaction, *Comput. Phys. Comm.*, **13** (1977), 149-155.
- [13] L. Chen, Stability and instability of solitary waves for generalized symmetric regularized-long-wave equation, *Phys. D*, **118** (1998), 53-68.
- [14] P.A. Clarkson, New similarity reductions and Painlevé analysis for the symmetric regularised long wave and modified Benjamin-Bona-Mahoney equations, *J. Phys. A*, **22** (1989), 3821-3848.
- [15] T. Dauxois and M. Peyrard, *Physics of Solitons*, Cambridge University Press, Cambridge, 2006.
- [16] X. Dong, Error estimates in the energy space for a Gautschi-type integrator spectral discretization for the coupled nonlinear Klein-Gordon equations, arXiv:1109.0765 [math-ph].
- [17] X. Dong, A trigonometric integrator pseudospectral discretization for the N-coupled nonlinear Klein-Gordon equations, *Numer. Algorithms*, **62** (2013), 325-336.
- [18] X. Dong, Z. Xu and X. Zhao: On time-splitting pseudospectral discretization for nonlinear Klein-Gordon equation in nonrelativistic limit regime, *Commun. Comput. Phys.*, **16** (2014), 440-466.
- [19] B. Guo, The spectral method for symmetric regularized wave equations, *J. Comput. Math.*, **5** (1987), 297-306.
- [20] W. Gautschi, Numerical integration of ordinary differential equations based on trigonometric polynomials, *Numer. Math.*, **3** (1961), 381-397.
- [21] E. Hairer, Ch. Lubich and G. Wanner, *Geometric Numerical Integration: Structure-Preserving Algorithms for Ordinary Differential Equations*, Springer, Berlin, 2006.
- [22] E. Hairer and Ch. Lubich, Long-time energy conservation of numerical methods for oscillatory differential equations, *SIAM J. Numer. Anal.*, **38** (2000), 414-441.
- [23] V.G. Makhankov, Dynamics of classical solitons (in nonintegrable systems), *Phys. Rep. C*, **35** (1978), 1-128.
- [24] K.W. Morton and D.F. Mayers, *Numerical Solution of Partial Differential Equations*, 2nd Edition, Cambridge University Press, Cambridge, 2005.

- [25] T. Ogino and S. Takeda, Computer simulation and analysis for the spherical and cylindrical ion-acoustic solitons, *J. Phys. Soc. Jpn.*, **41** (1976), 257-264.
- [26] C.E. Seyler and D.L. Fenstermacher, A symmetric regularized-long-wave equation, *Phys. Fluids*, **27** (1984), 4-7.
- [27] J. Shen, T. Tang and L. Wang, Spectral Methods: algorithms, analysis and applications, Springer-Verlag, Berlin Heidelberg, 2011.
- [28] Y. Shang, B. Guo and S. Fang, Long time behavior of the dissipative generalized symmetric regularized long wave equations, *J. Partial Differ. Equ.*, **15** (2002), 35-45.
- [29] A. Soffer and M.I. Weinstein, Multichannel nonlinear scattering for nonintegrable equations, *Commun. Math. Phys.*, **133** (1990), 119-46.
- [30] T. Wang and X. Zhao, Optimal l^∞ error estimates of finite difference methods for the coupled Gross-Pitaevskii equations in high dimensions, *Sci. China. Math.*, **57** (2014), 2189-2214.
- [31] T. Wang, L. Zhang and F. Chen, Conservative schemes for the symmetric Regularized Long Wave equations, *Appl. Math. Comput.*, **190** (2007), 1063-1080.
- [32] T. Wang and L. Zhang, Pseudo-compact conservative finite difference approximate solution for the symmetric regularized long wave equation, *Acta Math. Sci. Ser. A*, **26** (2006), 1039-1046.
- [33] B. Yan and L. Zhang, Symmetric Regularized Long Wave Equations, *Acta Math. Appl. Sin. Engl. Ser.*, **3** (2012), 458-470.
- [34] X. Zhao, On error estimates of an exponential wave integrator sine pseudospectral method for the Klein-Gordon-Zakharov system, *Numer. Methods Partial Differential Equations*, in press (2015), DOI: 10.1002/num.21994.
- [35] J. Zheng, Z. Zhang and B. Guo, The Fourier pseudospectral method for the SRLW equation, *Appl. Math. Mech.*, **10** (1989), 843-852.